

# Accurate Modelling of Monotron Oscillations in Small and Large Signal regimes

J.C. Cai, I. Syratcev, G. Burt

**Abstract—** In Klystron amplifiers, monotron oscillations may cause unacceptable beam instabilities. To facilitate fast and accurate analysis of such processes, rather than performing time-consuming Particle-in-Cell simulations, the theory of the monotron oscillations has been further developed for the small and large signal regimes and implemented into the klystron computer code KlyC. This development includes full considerations of the space charge effects, relativistic effects and can operate with arbitrary field distributions of the resonant mode. The effectiveness of these methods, have been demonstrated through benchmarking against PIC codes and has shown good (at 1% level) agreement, whilst KlyC computation time is significantly (at least 100 times) faster than in the PIC simulations.

**Index Terms—**Modelling, Monotron, Oscillation, Klystron.

## I. INTRODUCTION

A monotron oscillator is a simple linear beam electron device which utilizes the longitudinal beam-wave interaction to generate the self-excited microwave power, when continuous electrons move linearly with an initially constant velocity [1~3]. Coherent microwave radiation from a resonant cavity generated by these oscillations has made the monotron oscillator the simplest RF source since its discovery.

Large numbers of theoretical and experimental studies have been performed in the past in attempt to develop a comprehensive understanding of such transient radiation processes. A very basic analytical model, based on the assumption of an idealized gridded cavity gap, was initially used for the theoretical investigation of such transient radiation phenomenon. To simplify the analytical derivations, a non-relativistic electron beam without space charge effects has been taken into account and has been used in the original studies [4, 5]. Such a model can predict the onset of the monotron oscillation by calculating the beam transit angle and is useful for qualitative analysis. The extended theoretical model for the small signal regime was developed next and included the space charge effects [6~9]. It significantly improved the accuracy of threshold current calculation. Further modifications concerned the arbitrary electric field distribution in the resonant cavity [10,11] and relativistic effects [12,13]. However, the relativistic effects were associated only with the beam dynamics, without taking the space charge field into account, thus making the

results inaccurate. The large signal theory of the monotron oscillation was later targeted to simulate the RF power production in the regime when the beam current exceeds the threshold value. Such a process is very nonlinear and to make these simulations the space charge effects were ignored to simplify the theoretical model [14]. Particle-In-Cell (PIC) computer codes are the most accurate tools for the simulation of all types of the electron devices, including monotron oscillator [15,16]. Design efforts on the monotron oscillator with simplified RF structure topology were carefully conducted in the PIC simulations, demonstrating that optimized device can deliver RF power with an efficiency up to 20% [17,18]. It was also reported [19] that with a more complicated RF circuit, the efficiency can be further increased up to 50% in PIC simulations.

In high-power klystron amplifiers, the monotron oscillation is a parasitic effect as absolute instability, which can destroy the RF power generation. Thus, such instabilities should be studied and excluded at the early stage of klystron design [20,21]. For most klystrons, which adopt single gap cavities in the RF circuit, the threshold current of the monotron oscillation is usually rather high, since the effective impedance ( $R/Q \bullet M^2$ ) of the oscillation mode is much smaller than the one of the operating mode. However, in the multi-cell coupled structures used in Extended Interaction Klystrons (EIK), for the high frequencies range, the mode competition can become an issue [22~26]. The studies into high power, high efficiency and high frequency klystrons at CERN implied the use of the multi-cell cavities in the bunching circuit to compensate for the lack of impedance in the structure with large beam aperture [27].

In this paper, the hypothetical design of the high power (40 MW), 24 GHz klystron is considered. The klystron beam parameters (400 kV and 190 A) for this tube were chosen anticipating that 50% RF power production efficiency can be reached in this device with perveance of  $0.75 \mu\text{AV}^{-1.5}$ . In the initial optimization of the bunching cavities, it was concluded that three coupled cells operating in the  $\pi$  mode provided sufficient impedance, beam coupling and mode separation. At this stage, the cell period and gap length were adjusted to maximize the beam coupling, thus ensuring a sufficiently large frequency detuning of the bunching cavities in order to maintain the reasonable klystron bandwidth. Next, the cavity triplet was examined using the PIC code CST/3D operating with DC beam. It was found that a monotron oscillation is excited after a few hundred nanoseconds at the frequency corresponding to the  $\pi/2$  mode of the cavity triplet. Later, this effect was mitigated by

Jinchi Cai ([jinchi.cai@cern.ch](mailto:jinchi.cai@cern.ch)) and Graeme Burt are with Department of Engineering of Lancaster University, LA1 4YW, Lancaster, United Kingdom; Igor Syratcev ([igor.syratcev@cern.ch](mailto:igor.syratcev@cern.ch)) is with BE/RF group at CERN (European Organization for Nuclear Research), 1211, Geneva 23, Switzerland.

modifying the triplet topology (cell period and gap length). However, the re-optimization process appeared to be rather time consuming, as it involved massive simulations using a PIC code.

The large signal computer code for klystron simulations KlyC [28,29] has recently been developed at CERN. To facilitate fast and reliable simulations of the monotron oscillation using small and large signal regimes, a new dedicated module has been developed and implemented into the KlyC. In the process, the theory of monotron oscillations has been revised and completed with full consideration of space charge effects, relativistic effects and arbitrary electric field patterns, which are all calculated in a self-consistent manner. Particle-in-Cell computer codes are the most reliable tools for the study of beam-wave interaction problems. However, because of the transient nature of monotron oscillations, accurate system analysis, especially in the vicinity of its threshold parameters, using PIC codes becomes impractical, as the simulation time to reach the steady state will become unacceptable long. When compared to the time-consuming PIC simulations, the KlyC simulations based on these theoretical methods are much faster (almost 100 times) and accurate.

This paper is comprised of four sections. In Section II, the self-consistent small signal theory is derived from the general beam-wave interaction equations in a resonant cavity. In Section III, a large signal theory based on the modified algorithm previously developed for the klystron numerical simulation is demonstrated. In Section IV, the developed theoretical model for monotron oscillations is benchmarked against the PIC simulations, using various parameters sets of the 24 GHz triplets as examples. The conclusion is made in Section V.

## II. SMALL SIGNAL THEORY

The mathematical methods developed for KlyC (a large signal computer code for the klystron simulations) have been adopted as the premise for the small signal theory of resonant cavities with beam loading effects. To simplify the analytical derivations, a one-dimensional (1-D) approximation has been used, in which the particle trajectory and impedance of the RF cavity do not have radial dependence. In such approximation, DC (direct current) space charge effect can also be neglected. In the small signal regime, only fundamental harmonics need to be taken into account as a result of the linear approximation, whereas the whole system is dominated by the DC state.

Consider a resonant cavity, fed by a waveguide with waveguide mode voltages at the input and output,  $V_-$  and  $V_+$ , at the interface between the waveguide and the cavity, at a distance  $L$  between the reference plane and the interface. In 1D approximation, the mode excitation voltage in the resonant cavity can be written as [28]:

$$\sqrt{\frac{Q_{ext}\eta_0}{Z}}(V_-e^{j\beta L} + V_+e^{-j\beta L}) = V \quad (1a)$$

$$\frac{V}{\eta_0}\left(\frac{1}{Q_{in}} + 2j\frac{\omega - \omega_0}{\omega_0}\right) + \frac{N}{\sqrt{k_0}} \int_{z_1}^{z_2} \mathbf{I}_z(z) \cdot \mathbf{e}_z(z) dz \quad (1b)$$

where  $Q_{ext}$  and  $Q_{in}$  are the external and intrinsic quality factors of the resonant mode,  $\eta_0$  is free space wave impedance,  $Z$  and  $\beta$  are the wave impedance and phase advance of the propagating mode in the output waveguide,  $\omega_0$  is the resonant angular frequency of the mode  $k_0 = \omega_0/c$  and,  $\omega$  is the operating angular frequency. The position of the reference plane is determined by the condition that at this position, the wave amplitude will reach its maximum at the same time as the cavity's electric field.  $N$  is the number of beamlets if multi-beam Klystron is concerned.  $z_2 > z_1 > 0$  determines the integral region of the resonant mode.  $\mathbf{I}_z(z)$  is RF modulated current density of the electron beam at operating frequency.  $\mathbf{e}_z(z)$  is the longitudinal components of normalized eigen field of the resonant mode, which can be defined as:

$$E_{mz}(z) = V k_0^{\frac{1}{2}} e_z(z) \quad (2a)$$

$$\mathbf{e} = \frac{\mathbf{E}_m}{\sqrt{\iiint \mathbf{E}_m \cdot \mathbf{E}_m dV}} = \frac{\mathbf{E}_m}{\sqrt{2W_e/\epsilon_0}} \quad (2b)$$

where  $E_{mz}(z)$  is the electric field of the cavity mode and  $\mathbf{e}$  is the normalized value of that field.  $\mathbf{E}_m$  and  $W_e$  are the peak electric field and stored energy of the cavity mode, respectively.

Aside from the electric field of the resonant mode, an RF space charge field will be induced when the beam current is modulated. According to the simplification method used in [30], the 1-D space charge field can be express as:

$$E_{sz}(z) = -\frac{I_z(z) F^2}{j\omega\epsilon_0 S \gamma^2}$$

$$F^2 = 1/[1/\gamma^2 + (\frac{\mu_{0n} v_e}{\omega r_c})^2] \cdot \sum_{n=1}^{\infty} \frac{1}{(r_2^2 - r_1^2)^2} \left[ \frac{2}{\mu_{0n}} \frac{r_2 J_1(\mu_{0n} \frac{r_2}{r_c}) - r_1 J_1(\mu_{0n} \frac{r_1}{r_c})}{J_1(\mu_{0n})} \right]^2 \quad (3)$$

where  $E_{sz}(z)$  is the RF space charge electric field at position  $z$ ,  $I_z(z)$  is the modulated current density at position  $z$ ;  $r_1$ ,  $r_2$  and  $r_c$  are the inner beam, outer beam and the tunnel radii respectively. Here,  $\mu_{0n}$  is  $n^{\text{th}}$  root of 0-order Bessel function and  $\gamma$  is the Lorentz factor that contributes to the longitudinal contraction [31].  $S$  is the cross-sectional area of beam and  $v_e$  is the beam velocity.  $F > 0$  is a geometrical factor of the space charge effect. It should be noted, that relativistic effects are included in Eq. (3). The arrival functions the for electrons in one RF period can be solved from the beam dynamic equations [28], together with the linear approximation of the small perturbation of the particles velocities along their trajectories:

$$t(t_0, z) - t_0 - \frac{z}{v_e} = \eta_{e0} v_e^{-3} \gamma^{-3} \cdot \text{Im} \left( e^{j\omega t_0} \int_0^z dx \int_0^x (E_{mz1}(y) + E_{sz1}(y)) e^{j\beta_e y} dy \right) \quad (4)$$

where the emission plate for all electrons is  $z=0$ ,  $\eta_{e0}$  is the mass to charge ratio of electron,  $\beta_e = \omega/v_e$ . The arrival time  $t$  of electrons departing at  $t_0$  can be solved using Eq. (4). The modulated current can be calculated with the knowledge of arrival function by the integral method in [28]. The differential form can be rewritten as:

$$\eta_{e0} v_e^{-3} \gamma^{-3} \omega I_{z0} (E_{mz1}(z) + E_{sz1}(z)) = -j\beta_e^2 I_{z1}(z) - 2\beta_e \frac{dI_{z1}(z)}{dz} + j \frac{d^2 I_{z1}(z)}{dz^2} \quad (5a)$$

$$I_{z1}(0) = 0, \frac{dI_{z1}}{dz}(0) = 0 \quad (5b)$$

where  $I_{z0} < 0$  is the emission DC current. By combining Eq. (3) and Eq. (5a), the ordinary differential equation can be expressed as:

$$- \alpha(\gamma) \beta_e G_0 E_{mz}(z) = -j(\beta_e^2 - \beta_q^2) I_z(z) - 2\beta_e \frac{dI_z(z)}{dz} + j \frac{d^2 I_z(z)}{dz^2} \quad (6)$$

where

$$\alpha(\gamma) = \frac{1}{\gamma} \frac{1}{1 + \gamma}$$

$$\beta_q = \beta_e F \gamma^{-\frac{5}{2}} \frac{\omega_p}{\omega} > 0$$

$$\omega_p^2 = \frac{-I_{z0} \eta_{e0}}{\pi(r_2^2 - r_1^2) \epsilon_0 v_e}$$

and  $\omega_p > 0$  is the plasma angular frequency,  $G_0 = -I_{z0}/U_0 > 0$  is the ratio between beam current and beam voltage. With use of Eq. (5b) as the initial conditions and the fact that there is no field from  $0 < z < z_1$ , the modulated current can be solved in the cavity gap region  $z_1 < z < z_2$  as:

$$I_{z1}(z) = j\alpha(\gamma) \beta_e G_0 e^{-j(\beta_e + \beta_q)z} \cdot \int_{z_1}^z dx e^{2j\beta_q x} \int_{z_1}^x E_{mz}(y) e^{+j(\beta_e - \beta_q)y} dy \quad (7)$$

By combining Eq. (1b), Eq. (2a) and Eq. (7), the mode excitation equation can be derived as:

$$\sqrt{\frac{1}{Q_{ext} \eta_0 Z}} (V_- e^{j\beta L} - V_+ e^{-j\beta L}) = \quad (8)$$

$$\frac{V}{\eta_0} \left( \frac{1}{Q_{in}} + Y_e \rho + 2j \frac{\omega - \omega_0}{\omega_0} \right)$$

where  $Y_e$  and  $\rho$  are the beam-loading admittance and mode characteristic impedance respectively, defined as:

$$Y_e = G_e + jB_e = NjG_0 \alpha(s) \beta_e / \left( \int_{l_0+L_1}^{l_0} |f(z)| dz \right)^2 \cdot e^{-j(\beta_e + \beta_q)(z - z_1)} f(z) dz \cdot \int_{z_1}^{z_2} \int_{l_0}^z e^{2j\beta_q(x-l_0)} dx \int_{l_0}^x f(y) e^{+j(\beta_e - \beta_q)(y-l_0)} dy \quad (9a)$$

$$\rho = \eta_0 \left| \frac{e_{zm} \int_{l_0}^{l_0+L_1} |f(z)| dz}{\sqrt{k_1}} \right|^2 = \frac{V_{gm}^2}{2\omega_1 W} \quad (9b)$$

in which the  $f(z)$  indicates the relative variation principle of normalized  $e_z(z)$ :

$$e_{zm} = \mathbf{max} |e_z(z)| \quad f(z) = e_z(z) / e_{zm} \quad (10)$$

In the small signal assumptions, the beam loading effect can equivalently change the quality factor and resonant frequencies, with combination of Eq. (8) and Eq. (9):

$$\sqrt{\frac{1}{Q_{ext} \eta_0 Z}} (V_- e^{j\beta L} - V_+ e^{-j\beta L}) = \frac{V}{\eta_0} \left( \frac{1}{Q_{in}} + \frac{1}{Q_{beam}} + 2j \frac{\omega - \omega_0(1 + \delta_{beam})}{\omega_0} \right) \quad (11)$$

$$\frac{1}{Q_{beam}} = \rho G_e, \delta_{beam} = -\frac{1}{2} \rho B_e$$

With combination of Eq. (1a) and Eq. (11), the small signal theory for the input cavity of klystron is completed. When the monotron oscillation is concerned, the propagating mode at the waveguide port should be only in one direction (free radiation), thus  $V_- = 0$ . With such a condition, the oscillation will not build up, if the small signal is decaying with a positive loaded quality factor:

$$\frac{1}{Q_{load}} = \frac{1}{Q_{ext}} + \frac{1}{Q_{in}} + \frac{1}{Q_{beam}} \quad (12)$$

The threshold condition for the instability will then be reached when  $1/Q_{load} = 0$ , thus:

$$\frac{1}{Q_{beam}} = \rho G_e = -\frac{1}{Q_{ext}} - \frac{1}{Q_{in}} \quad (13)$$

The beam loading conductance ( $G_e$ ) depends on the electric field distribution (Eq. 9a). To trigger an oscillation, the value of  $G_e$  should be negative and the beam current should be high enough to exceed the threshold. The calculation of the threshold

current is based on the solution of such nonlinear equations. When the space charge is neglected, the threshold current can be calculated analytically, since  $G_e$  is proportional to  $G_\rho$ . The onset oscillation frequency can be solved together with the threshold current.

### III. LARGE SIGNAL THEORY

When the beam current exceeds the threshold, microwave radiation will be generated and it will interact with the electron beam in a nonlinear manner [32]. In such situations, the monotron oscillation frequency and generated RF power level could be solved for the steady state of the system operation. An initial estimation of the oscillation frequency can be done using the small signal theory. Such a frequency can be adopted as a tentative operating frequency and can be used as a driving frequency in the KlyC klystron-type large signal simulations. The actual frequency of the oscillation will be slightly different, but this difference is within the fraction of a percent (see the next chapter). With such a small detuning, the beam dynamics, the beam current modulation process and the space charge field excitation by the modulated beam will be barely affected. At the same time, the electric field amplitude of the resonant mode strongly depends on the difference between the mode frequency and the beam current modulation frequency. In the simulations, the operating frequency used for the beam modulation will be kept constant, whilst the value of the oscillation frequency responsible for the resonant mode excitation in Eq. (1.2) will be solved together with the electric field amplitude. The convergent solution for the steady state oscillation requires that the RF phase has to be fixed at some arbitrary angle. If this angle is set to be zero, the excited mode voltage amplitude will be a positive real number. In simulations, the initial modulating mode voltage in the cavity (Eq. (2.1)) is set to be 10% of the beam voltage. At the first iteration, when the beam modulation and the space charge field excitation are solved, the oscillation angular frequency  $\omega'$  for the next iteration is modified in a way, so that the cavity voltage amplitude remains as a positive real number:

$$\frac{2 \frac{\omega' - \omega_0}{\omega_0}}{1/Q_{in} + 1/Q_{ext}} = - \frac{\text{imag} \int_{z_1}^{z_2} \mathbf{I}_z(z) \cdot \mathbf{e}_z(z) dz}{\text{real} \int_{z_1}^{z_2} \mathbf{I}_z(z) \cdot \mathbf{e}_z(z) dz} \quad (14)$$

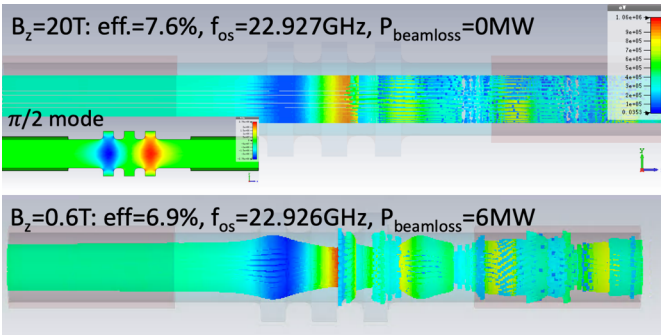


Fig. 1. Beam modulation caused by the monotron oscillation in the triplet for different magnetic focusing field amplitudes. Snapshots have been done at 300ns of the simulation time.

With this oscillation frequency modification, the updated value of the mode voltage will be calculated. Such an iterative process will converge to some steady state values of the cavity mode voltage and oscillation frequency.

When the beam current is below the threshold, the large signal simulations in KlyC will not yield a convergent solution. Through the iterations, the mode voltage will be exponentially decaying in attempt to approach zero value. Thus, the threshold current can be estimated in the large signal simulations by sweeping the beam current value in some discrete sequence. The KlyC can only simulate the converged parameters of the system in steady state for the case where the particles do not experience any radial movement. Accurate simulations of the monotron oscillation transient processes including radial beam expansion in the presence of the focusing magnetic field can be done using PIC codes. However, it is impractical to use the PIC codes to obtain the accurate value of the threshold current, as the simulation time will be increasing exponentially, when the beam current will be approaching the threshold value.

### IV. MODEL VERIFICATION

To illustrate the application of the developed methods for monotron oscillation simulations, the hypothetical design of a high power (40 MW), 24 GHz klystron is considered. The klystron beam parameters are: 400 kV and 190 A. In the initial optimization of the bunching cavities, it was concluded that three coupled cells with the period of 5.8mm and 2.5 mm gap, operating in the  $\pi$  mode, provided the highest effective impedance and sufficient modes separation. However, the adjusted 0 and  $\pi/2$  modes in such a circuit will be presented. These modes will not participate in the beam bunching process, because of the sufficient frequency detuning, but they could be dangerous, if their electric field patterns can satisfy, at certain beam voltage and current, the conditions of the monotron oscillation excitation. The dedicated simulations using CST/3D PIC computer code [33] for the stand along triplet and DC beam configuration have been done to verify the problem. It was found, that monotron oscillation was excited and stabilized after 300 ns. The simulations have been done for the cases of large solenoidal magnetic field (20 T), providing the ‘frozen’ beam condition and moderate magnetic field amplitude of 0.6 T (3.5xBrilluoin field) resulting in a radial beam expansion and beam losses, see Fig. 1. However, for both cases the oscillation

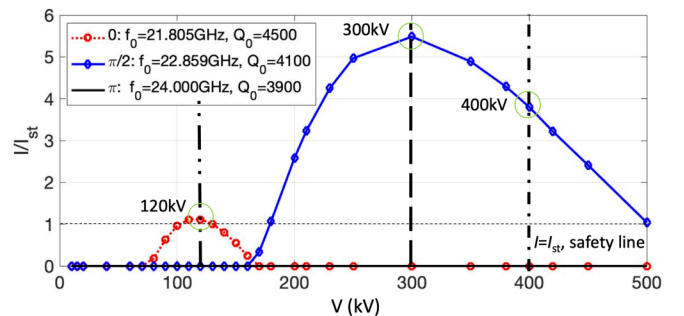


Fig. 2. Small signal analysis of the triplet for the different beam voltages.  $TM_{010}$  0,  $\pi/2$ ,  $\pi$  modes are considered.

frequency is almost identical (22.926(7) GHz) and is close to the  $TM_{010}-\pi/2$  mode frequency of the triplet (22.859 GHz). Also, the beam-to-RF power extraction efficiencies are close enough (7.6% cf. 6.9%) despite the heavy beam losses for the case with 0.6 T magnetic field amplitude. Therefore, the ‘frozen’ beam assumption adopted by KlyC was expected to be accurate enough for the monotron oscillation analysis.

The internal KlyC EM module allows the calculation of the eigen frequencies and eigen fields of the individual and coupled cavities, which facilitates rapid small signal analysis in KlyC [29]. For  $TM_{010}-\pi/2$  mode, the predicted threshold current was 50.7A with oscillation onset frequency of 22.873 GHz. This confirmed, that the system shall be unstable, when the beam current is 190A. The threshold current was next calculated for all three modes of the triplet using the small signal theory approximations, see Fig. 2. In these calculations, the beam current ( $I$ ) for the different beam voltages ( $V$ ) is calculated for the fixed beam perveance of  $0.75 \mu AV^{-1.5}$ . In Fig. 2,  $I_{st}$  is the value of threshold current predicted by the small signal theory. When the beam current  $I$  is larger than  $I_{st}$ , the monotron oscillation will be excited. This analysis concluded, that for the operating  $TM_{010}-\pi$  mode the beam loading quality factor is always positive in the range of applied beam voltages. For the other two modes, the monotron oscillation can be excited in their specific ranges of the beam voltages.

The large signal simulations have been done with KlyC/1.5D and CST/3D for three specific (see Fig. 2) values of the beam

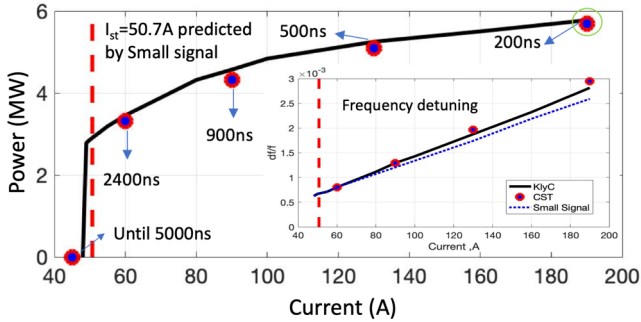


Fig. 3. Comparison between KlyC large & small signal simulations (solid and dash lines) and CST/3D PIC simulations (circles) for the beam voltage 400kV. The time labels on the plot correspond to the onset time of the monotron oscillation in the PIC simulations.

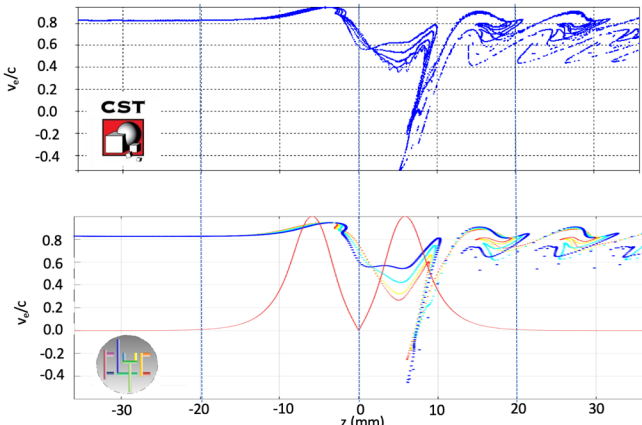


Fig. 4. The photographs of the particles phase space calculated in CST/3D (top) and KlyC (bottom) for the operating point with  $V=400kV$  and  $I=190A$ .

voltage: 120 kV, 300 kV and 400 kV. In Fig. 3 the KlyC/1.5D ( $TM_{010}-\pi/2$ ) and CST/3D results at 400kV are compared for the different beam current. The RF power extracted from the beam and the oscillation frequency detuning are in a good agreement (1% level) between two codes. The particles phase space plots simulated in KlyC/1.5D and CST/3D (steady state) are shown in Fig. 4. As indicated in Fig. 3, the oscillation onset time is increasing in PIC simulations, when the beam current is approaching the threshold value. The same time, in the KlyC large signal simulations, the number of iterations needed to reach the specified level of the solution convergence is also increased. The KlyC convergence processes for the cases of beam current below and above threshold are illustrated in Fig. 5. PIC simulations of the monotron oscillation are rather time consuming. For example, with the beam current of 190 A, it takes almost two days to reach the steady state in CST/3D simulations using ‘office’ PC with 3.4GHz processors, 4 cores CPU and 8 GB RAM. To simulate 2400 ns at 60 A it will take three weeks, whilst with KlyC/1.5D, it will take about 10 minutes. Therefore, it is impractical to use the PIC codes for the accurate simulation of the oscillation threshold current, because there will be no guaranty that oscillation onset time is shorter than the time limit imposed by the user in simulations. Contrary, in the KlyC/1.5D large signal simulations, the threshold current can be measured with good accuracy through the series of discrete simulations for the different beam current. In these simulations it was found, that the actual value of threshold current is 3.5% lower than the one predicted using the small signal approximation (49A cf. 50.7A). The oscillation frequencies predicted in the small and large signals simulations are very close, the discrepancy measured at 190 A is about 0.03%, see Fig. 3. The results of simulations for the cases of

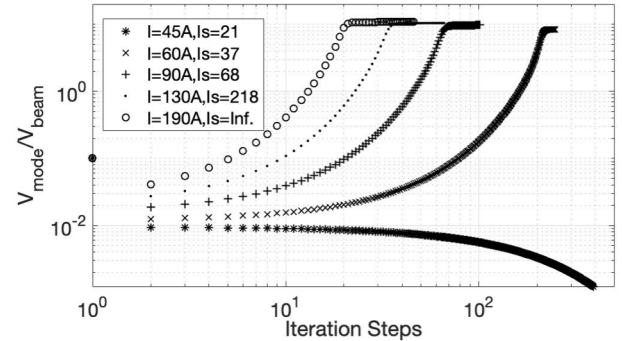


Fig. 5. The normalized mode voltages convergence as functions of the iteration steps in KlyC/1.5D simulations for the different beam current ( $V=400kV$ ).

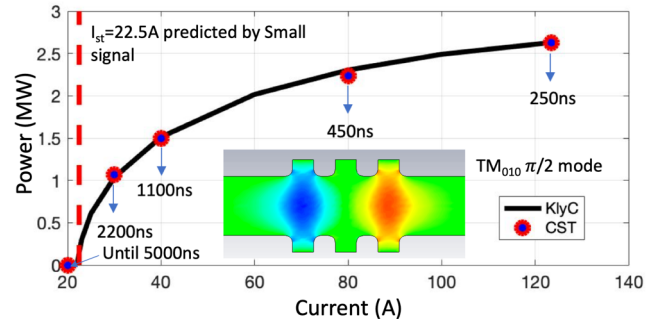


Fig. 6. Benchmark between KlyC large signal simulation (solid line) and CST/3D simulation (circles) for the beam voltage 300kV.

300kV (TM<sub>010</sub>- $\pi/2$  mode) and 120kV (TM<sub>010</sub>-0 mode) are shown in Fig. 6 and Fig. 7. Once again, good agreement between KlyC/1.5 large signal simulations and CST/3D has been observed. The particles phase space plots simulated in KlyC/1.5D and CST/3D (steady state) for 120 kV and 40 A beam (TM<sub>010</sub>-0 mode) are shown in Fig. 8.

The developed technique has been used to mitigate monotron oscillations in the 24 GHz cavity triplet. Throughout the post-optimization in KlyC/1.5D, it was found that the most crucial geometrical parameter is the cells period, as it imposes the strong influence on the electric field distribution of the modes. Finally, the 3-cell structure with a cell period of 3.8 mm has been adopted, due to the fact that it provided suppression of the monotron oscillation ( $I/I_{st} < 1$ ) in the beam voltage range up to 500 kV, see Fig. 9. For the klystron operating point ( $V=400$  kV,

$I=190$  A), the triplet has been simulated in CST/3D up to 5000 ns and no monotron oscillation has been found. Such a result gives a sufficient margin for the possible oscillation onset time, as the klystron is expected to operate with 1000 ns RF pulses. As a drawback of such modification, the effective impedance of the operating TM<sub>010</sub>- $\pi$  mode was reduced by 30%. This will affect (reduce) the frequency bandwidth of the device.

## V. CONCLUSION

The theory of monotron oscillations in linear beam devices was carefully reviewed and further developed for the small and large signals regimes. It was successfully implemented into the CERN made klystron computer code KlyC. This development includes full considerations of the space charge effects, relativistic effects and can operate with arbitrary field distribution of the resonant mode. The effectiveness of the methods, both, for the analytical small signal theory and numerical large signal simulations, was demonstrated through the benchmarking against the PIC code CST/3D. This comparison showed good (at 1% level) agreement between the two codes, whilst KlyC computation time is significantly faster (at least 100 times) than the PIC simulations. Although, PIC simulation will still be necessary at the final stage in order to investigate the effect of the realistic magnetic field. The developed methods can be used not only for klystron analysis, but also for the independent study and optimization of the Monotron as an RF power generator.

## REFERENCES

- [1] R.K. Parker, R.H. Abrams, B.G. Danly, B. Levush "Vacuum electronics", *IEEE Trans. On Microwave Theory and Techniques*, vol.50 no.3, pp.835-845, March 2002.
- [2] J. Müller, "Electron oscillations in high vacuum", *Hochfrequenztech. u. Elektroakustik*, vol.41, pp. 156-157, May 1933.
- [3] F. B. Llewellyn and A. E. Bowen, "The production of ultrahigh frequency oscillations by means of diodes", *Bell Syst. Tech. J.*, vol. 18, no. 2, pp. 280-284, 1939.
- [4] J. J. Müller and E. Rostas, "Un Générateur a Temps de Transit, Utilisant un Seul Résonateur de Volume", *Helv. Phys. Acta* vol. 13, no. 3, pp. 435-450, 1940.
- [5] E.J. Graig, "The beam-loading admittance of gridless klystron gaps", *IEEE Trans. on Electron devices*, vol.145, no.4, pp.273-278, May 1967.
- [6] D.L. Webster, "Theory of Klystron oscillations", *J. Appl. Phys.*, vol. 10, no. 12, pp. 864-872, 1939.
- [7] S. Ramo, "charge and Field Waves in an Electron Beams", *Phys. Rev.*, Vol. 56, no.3, pp. 276-283, 1939.
- [8] W.C. Hahn, "Small signal Theory of Velocity Modulated Electron Beams", *Gen. Elect. Rev.*, Vol.42, no.6, pp. 258-270, 1939.
- [9] G.M. Branch, "Electron beam coupling in interaction gaps of cylindrical symmetry," *IRE Transactions on Electron Devices*, vol. 8, no. 3, pp. 193-207, 1961.
- [10] Y.G. Ding, "Theory and Computer Simulation of High power Klystron," National Defense Industry Press, 2008.
- [11] W.C. Lu, Y.G. Ding, W. Yong, "The theory and computer simulation of beam-loading conductance in the double-gap coupled cavity," *Acta, Phys. Sin.*, Vol.16, No.12, pp. 128401, 2011.
- [12] E.J. Craig, "Relativistic beam-loading admittance", *IEEE Transactions on Electron Devices*, Vol. 16, no. 1, pp. 139-139, 1969.
- [13] G. Nusinovich, M. Read, and L.Q. Song, "Excitation of monotron oscillation in klystrons", *Phys. of Plasma*, Vol. 11, No. 11, pp. 4893-4903, 2004.
- [14] V. K. Yulpatov, "The excitation of oscillations in a cavity resonator by means of a relativistic electron beam", *Radiophysics and Quantum Electronics*. Vol. 13, No. 12, pp 1374-1377, December 1970.

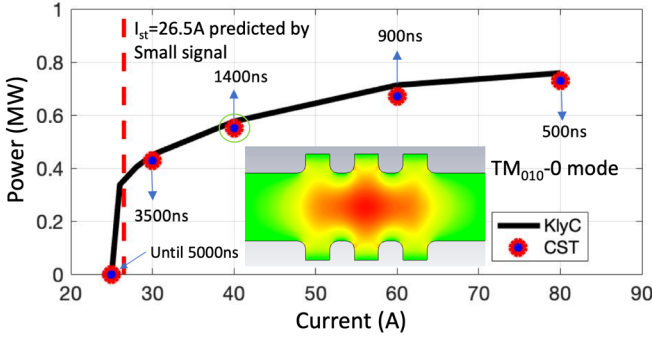


Fig. 7. Comparison between KlyC large & small signal simulations (solid and dash lines) and CST/3D PIC simulations (circles) for the beam voltage 120kV. The time labels on the plot correspond to the onset time of the monotron oscillation in the PIC simulations.

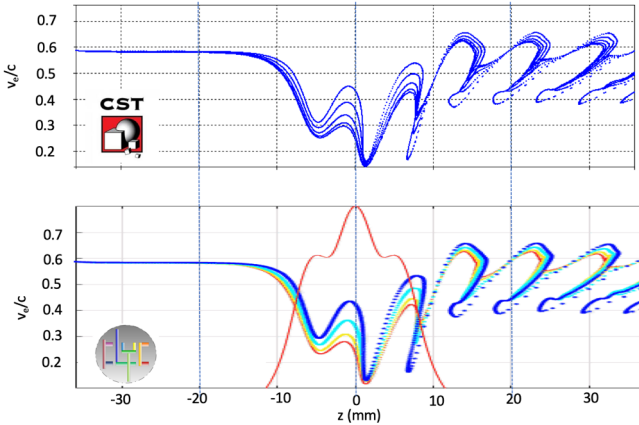


Fig. 8. The photographs of the particles phase space calculated in CST/3D (top) and KlyC (bottom) for the operating point with  $V=120$  kV and  $I=40$  A.

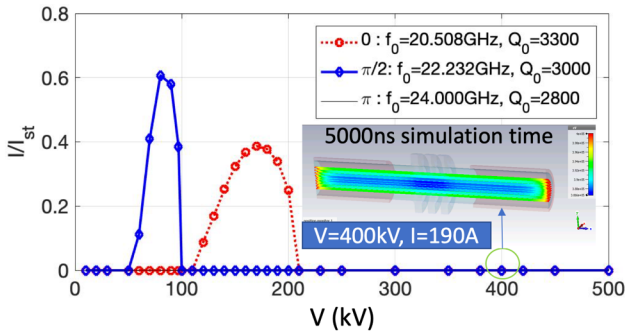


Fig. 9. Small signal analysis of the triplet with 3.8mm cells period for the different beam voltages. TM<sub>010</sub> 0,  $\pi/2$ ,  $\pi$  modes are considered.

- [15] G.B. Wilsen, J.W. Luginsland, Y.Y. Lau, T.M. Anotosen, D.P. Chernin, P.M. Tchou and L.D. Ludeking. "A simulation Study of Beam loading on a Cavity", *IEEE Transactions on Plasma Sciences*, Vol 30, No. 3, pp. 1160-1168, 2002.
- [16] B.M Marder, M.C. Clark, L.D. Bacon, J.M. Hoffman, R.W.Lemke and P.D. Coleman. "The split-cavity oscillator: A high-power e-beam modulator and microwave source", *IEEE transactions on plasma science*, vol. 20, no. 3 pp. 312-331, 1992.
- [17] J. J. Barroso, "A triple-beam 6.7 GHz, 340 kW monotron", *IEEE Trans. Electron Devices*, vol. 48, no.4, pp. 815-817, April 2001.
- [18] J. J. Barroso, "Design facts in the axial monotron", *IEEE Trans. Plasma Sci.* vol. 28, no. 3, pp. 652-656, 2000.
- [19] J. J. Barroso, "Stepped electric-field profiles in transit-time tubes", *IEEE Trans. Electron Devices*, May, vol. 52 no. 5 pp. 872-877, May 2005.
- [20] E. Wright, R. Callin, G. Caryotakis, K. Eppley, K. Fant, R. Fowkes, and R. Phillips, "Design of a 50-MW-klystron at X-band", *AIP Conference Proceedings*, Vol. 337, No. 1, pp. 58-66, July, 1995.
- [21] G. Caryotakis, "The klystron: A microwave source of surprising range and endurance", *Physics of Plasmas* vol. 5, no. 5, pp. 1590-1598, 1998.
- [22] S. Chen, C. Ruan, W. Yong, C. Zhang, D. Zhao, X. Yang and S. Wang, "Particle-in-cell simulation and optimization of multi-gap extended output cavity for a W-band sheet-beam EIK", *IEEE transactions on plasma science*, Vol. 42, No. 1, pp. 91-98, 2013.
- [23] S. Li, J. Wang, G. Wang and D. Wang, "Theoretical studies on stability and feasibility of 0.34 THz EIK", *Physics of Plasmas*, Vol. 24, No.5, pp. 053107, 2017.
- [24] A. Karp and G.T. Hunter, "Higher Order Modes and Instabilities in Coupled-Cavity TWTs", *IEEE Trans. on Electron devices*, vol.33, no.11, pp.1890-1895, November 1986.
- [25] S. Lu, C. Zhang, S. Wang and Y. Wang, "Stability Analysis of a Planar Multiple-Beam Circuit for W-band High-Power Extended-Interaction Klystron", *IEEE Trans. on Electron devices*, vol.62, no.9, pp.3042-3048, September 2015.
- [26] F. M. Lin and X.P. Li, "Monotron Oscillation in Double-Gap Coupling Output Cavities of Multiple-Beam Klystrons", in *IEEE Trans. on Electron devices*, vol.61, no.4, pp.1186-1192, April 2014.
- [27] J.C. Cai, I. Syratchev, "Modeling of coupled cell output structures for the Klystrons," *IEEE Trans. on Electron Devices*, vol.66 no.11, pp.4964-4969, November 2019.
- [28] J.C. Cai, I. Syratchev, "KlyC: 1.5D Large Signal Simulation Code for Klystrons", *IEEE Trans. on Plasma Science*, vol.47, no.4, pp.1734-1741, April 2019.
- [29] KlyC user manual. Available at : <http://cds.cern.ch/record/2649486/>.
- [30] J. C. Cai, I. Syratchev and Z. N. Liu, "Scaling Procedures and Post-Optimization for the Design of High-Efficiency Klystrons", *IEEE Trans. on Electron devices*, vol.66, no.2, pp.1075-1081, February 2019.
- [31] A. Jensen, G. Caryotakis, G. Scheitrum, D. Sprehn and B. Steele, "Sheet Beam Klystron Simulations Using AJDISK", in *IEEE Vacuum Electronics Conference*, Monterey, US, pp. 489-490, April 2016.
- [32] J.C. Cai, L.L. Hu, H.B. Chen, X. Jin, H. Chen, "Study on the increased threshold current in the development of 220-GHz Folded Waveguide Backward-Wave Oscillator", in *IEEE Trans. on Microwave theory and techniques*, vol.64, no.11, pp.3678-3685, November 2016.
- [33] CST 2018. Available at: <https://www.cst.com/products>.